PADOVA UNIVERSITY PRESS

Dolomites Research Notes on Approximation

Special Issue dedicated to Robert Schaback on the occasion of his 75th birthday, Volume 15 · 2022 · Pages 1–11

Interpolating sequences of 3D-data with C^2 quintic PH B-spline curves

Gudrun Albrecht[a] · Carolina Vittoria Beccari[b] · Lucia Romani[c,*]

Communicated by Francesco Marchetti

Abstract

The goal of this paper is to present an effective method for interpolating sequences of 3D-data by means of C^2 quintic Pythagorean-Hodograph (PH) B-spline curves. The strategy we propose works successfully with both open and closed sequences of 3D-points. It relies on calculations that are mostly explicit thanks to the fact that the interpolation conditions can explicitly be solved in dependence of the coefficients of the pre-image PH B-spline curve. In order to select a more suitable interpolant a functional is minimized in two remaining free coefficients of the pre-image PH B-spline curve and some angular parameters.

1 Introduction

The research activity on Pythagorean Hodograph (PH) curves has been especially focused on the quintic degree case (see, e.g., [2–13, 15–17]) and its generalization to the order-6 non-polynomial case (see, e.g., [14, 18–20]) due to the fact that such curves are known to offer flexible solutions to several types of interpolation problems. These range from the standard point interpolation [2, 6, 11, 12], to the interpolation of Hermite data [4–6, 8–10, 13–15, 17–20] or the interpolation of prescribed boundary points with the associated first derivatives and curvatures [3]. Several papers also dealt with interpolation subject to arc-length constraints such as, e.g., [7, 16]. Among the papers that considered the standard point interpolation problem, we here mention only those that constructed a globally C^2 PH interpolant, and do not dwell on those requiring the production of a curve with a certain length since this constraint is not considered in our work.

The focus of our paper is indeed on the problem of interpolating sequences of 3D-data that may be either open or closed (i.e. with the last point coinciding with the first). The type of PH quintic interpolants we aim at constructing is the spatial C^2 quintic PH B-spline curve that belongs to the general class of spatial Pythagorean-Hodograph B-Spline curves introduced in [2]. Since these curves may be constructed on either a clamped or a periodic knot partition, we describe the interpolation method for both the cases and point out its capability to efficiently single out an interpolant to both open and closed sequences of 3D-points.

Within the setting of C^2 PH spline interpolation of sequences of 3D data, the main features of our approach are the following:

- a conceptually simple construction of the interpolating curve;
- an easy to compute solution where the calculations of the pre-image coefficients are all explicit except for those related to the first two coefficients which require the minimization of a suitable functional.

Earlier papers which considered a similar context are [11], [12] and [13]. Compared to [11], in our work we consider two initial conditions (related to the choice of the first two coefficients of the pre-image) rather than an initial and a final condition as in [11]. In this way, by giving up the symmetry of the non-linear system with respect to the data, we obtain a non-linear system for the coefficients of the pre-image which is easier to be solved than the quadratic non-linear system in all the quaternion unknowns that is considered in [11]. More specifically, in our paper the first two coefficients of the pre-image are obtained by minimizing a suitable functional, whereas all the remaining coefficients are successively obtained by means of explicit quaternion formulas. Since the minimization of the functional not only depends on the first two coefficients of the pre-image, but also on the PH B-spline angular variables, the interpolation curve is produced globally and does not have a fully explicit forward local construction like in [13]. Finally, differently from [12], our approach does not rely on a reference curve to accomplish the construction of a good PH interpolant.

Our paper is organized as follows. In Section 2 we recall the needed background by referring the reader to our previous works. In Section 3 and Section 4 we formulate the interpolation problem by distinguishing between the clamped and the periodic case. In Section 5 we summarize the proposed interpolation method in algorithmic form, and we explain how to deal with its effective use by suggesting solutions to solve any practical concerns. Finally, in Section 6 we illustrate the performance of our interpolation method by exhibiting a number of numerical examples. Conclusions are drawn in Section 7.

[a] Escuela de Matemáticas, Universidad Nacional de Colombia, Sede Medellín, Colombia (galbrecht@unal.edu.co)
[b] Dipartimento di Matematica, Alma Mater Studiorum Università di Bologna, Italy (carolina.beccari2@unibo.it)
[c] Dipartimento di Matematica, Alma Mater Studiorum Università di Bologna, Italy (lucia.romani@unibo.it)

2 Notation and background material on our work

To keep the paper relatively short and avoid duplication of previously published material, we deliberately do not include details on the recently introduced class of spatial Pythagorean-Hodograph B-Spline curves. For a concise review of the key properties of non-uniform B-Spline basis functions (defined on both clamped and periodic partitions) and the resulting spline curves, the interested reader is referred to [1]. Additionally, for a general overview of spatial Pythagorean-Hodograph B-Spline curves, the reader can consult [2].

In the following, in order to have a common notation for describing our interpolation method in the case of a clamped as well as periodic PH B-spline curve $\mathbf{r}$, we will denote the underneath knot partition with $\boldsymbol{\rho}$ and the knots of $\boldsymbol{\rho}$ with either t_j or $\langle t_j\rangle^n$ depending if they are simple or with multiplicity $n>1$. Moreover, we will refer to the knot interval lengths specified by the previously mentioned knots of $\boldsymbol{\rho}$ with d_j. The control points of the PH B-spline curve $\mathbf{r}$ depend on the control points of its hodograph $\mathbf{r}'(t)=\mathbf{p}(t)$, which in turn depend on the quaternion coefficients $\mathcal{Z}_i$ of the B-spline quaternion pre-image curve $\mathcal{Z}(t)=\sum_{i=0}^{p}\mathcal{Z}_i N^2_{i,\boldsymbol{\mu}}(t)$ defined for $t\in[0,1]$ and $p\in\{m,m+2\}$, where m (resp. $m+2$) is the number of 3D-points to be interpolated by the clamped (resp. periodic) PH B-spline curve $\mathbf{r}(t)$. For further details on $\mathcal{Z}(t)$ and the nature of the knot partition $\boldsymbol{\mu}$ of the normalized B-spline functions therein we refer the reader to [1, 2]. Our interpolation conditions will depend on these quaternion coefficients $\mathcal{Z}_i$.

For the sake of shortness, we will also use the following abbreviations for denoting frequently encountered expressions of the knot intervals, for which the exact index ranges will be specified later (see Section 3 and 4 respectively). Precisely, from here on, for all $j>0$ we assume

$$\begin{aligned}\alpha_{1,j}&:=\frac{1}{6}\,\frac{d_j\,d_{j+1}}{(d_{j-1}+d_j)(d_j+d_{j+1})},\quad \alpha_{2,j}:=\frac{1}{6}\,\frac{(d_j)^2}{(d_{j-1}+d_j)(d_j+d_{j+1})},\\ \alpha_{3,j}&:=\frac{2}{3}+\frac{1}{3}\,\frac{d_{j-1}\,d_{j+1}}{(d_{j-1}+d_j)(d_j+d_{j+1})},\quad \alpha_{4,j}:=\frac{1}{6}\,\frac{d_{j-1}\,d_j}{(d_{j-1}+d_j)(d_j+d_{j+1})},\end{aligned}\tag{1}$$

and, for all $j\geq 0$, we additionally define

$$\beta_{1,j}:=\frac{d_{j+1}}{d_j+d_{j+1}},\quad \beta_{2,j}:=\frac{1}{2}\,\frac{d_j}{d_j+d_{j+1}}.\tag{2}$$

3 Formulating the interpolation problem for open sequences of 3D-data

Given a sequence of m 3D-points $\mathbf{c}_k$, $k=2,\ldots,m+1$ (where $m\geq 2$), we want to compute a C^2 clamped quintic PH B-spline curve

$$\mathbf{r}:\ [0,1]\to\mathbb{R}^3$$

that satisfies the conditions

$$\mathbf{r}(t_k)=\mathbf{c}_k\,,\ k=2,\ldots,m+1\,.\tag{3}$$

The knots t_k, $k=2,\ldots,m+1$ involved in the above interpolation constraints are chosen in accordance with the distribution of the interpolation points $\mathbf{c}_k$, e.g., by either uniform, chordal or centripetal parametrization. This amounts to computing first

$$\tau_0=0,\qquad \tau_i=\tau_{i-1}+\|\mathbf{c}_{i+2}-\mathbf{c}_{i+1}\|_2^{\theta},\quad i=1,\ldots,m-1\quad\text{with}\quad \theta\in\left\{0,\frac{1}{2},1\right\}$$

and then setting

$$t_k:=\frac{\tau_{k-2}}{\tau_{m-1}},\qquad k=2,\ldots,m+1.$$

Hence, the values of $t_2\equiv 0, t_3,\ldots,t_m,t_{m+1}\equiv 1$ are used to construct the clamped knot partition

$$\boldsymbol{\rho}:=\left\{\langle t_2\equiv 0\rangle^6,\,\{\langle t_i\rangle^3\}_{i=3,\ldots,m},\,\langle t_{m+1}\equiv 1\rangle^6\right\}$$

and the associated knot intervals

$$d_0=d_m:=0,\qquad d_i:=t_{i+2}-t_{i+1},\quad i=1,\ldots,m-1.$$

Since $t_2\equiv 0$ and $t_{m+1}\equiv 1$ are 6-fold knots in the partition $\boldsymbol{\rho}$, we have that the normalized quintic B-splines $N^5_{i,\boldsymbol{\rho}}(t)$, $i=0,\ldots,3m-1$ built upon $\boldsymbol{\rho}$ satisfy

$$N^5_{i,\boldsymbol{\rho}}(0)=\begin{cases}1, & \text{if } i=0\\ 0, & \text{otherwise}\end{cases}\qquad\text{and}\qquad N^5_{i,\boldsymbol{\rho}}(1)=\begin{cases}1, & \text{if } i=3m-1\\ 0, & \text{otherwise.}\end{cases}$$

This property implies that the border control points of the C^2 clamped quintic PH B-spline curve defined as (see [2, Section 3.2.1])

$$\mathbf{r}(t):=\sum_{i=0}^{3m-1}\mathbf{r}_i\,N^5_{i,\boldsymbol{\rho}}(t),\quad t\in[0,1]\tag{4}$$

are interpolated, i.e.,

$$\mathbf{r}_0=\mathbf{r}(0)=\mathbf{r}(t_2)=\mathbf{c}_2\,,\quad \mathbf{r}_{3m-1}=\mathbf{r}(1)=\mathbf{r}(t_{m+1})=\mathbf{c}_{m+1}\,.$$

As to the remaining control points of $\mathbf{r}(t)$, we assume them to satisfy the relations (see again [2, Section 3.2.1])

$$\begin{aligned}
\mathbf{r}_1 &= \mathbf{r}_0 + \frac{d_1}{5}\,\mathbf{p}_0,\\
\mathbf{r}_2 &= \mathbf{r}_1 + \frac{d_1}{5}\,\mathbf{p}_1,\\
\mathbf{r}_{3j} &= \mathbf{r}_{3j-1} + \frac{d_j}{5}\,\mathbf{p}_{3j-1}, \quad j=1,\dots,m-1,\\
\mathbf{r}_{3j+1} &= \mathbf{r}_{3j} + \frac{d_j+d_{j+1}}{5}\,\mathbf{p}_{3j}, \quad j=1,\dots,m-2,\\
\mathbf{r}_{3j+2} &= \mathbf{r}_{3j+1} + \frac{d_j+d_{j+1}}{5}\,\mathbf{p}_{3j+1}, \quad j=1,\dots,m-2,\\
\mathbf{r}_{3m-2} &= \mathbf{r}_{3m-3} + \frac{d_{m-1}}{5}\,\mathbf{p}_{3m-3},\\
\mathbf{r}_{3m-1} &= \mathbf{r}_{3m-2} + \frac{d_{m-1}}{5}\,\mathbf{p}_{3m-2},
\end{aligned} \tag{5}$$

where $\mathbf{r}_0$ is an arbitrary 3D-point and

$$\begin{aligned}
\mathbf{p}_{3j-1} &= \alpha_{1,j}\,(\mathcal{Z}_{j-1}\,\mathbf{i}\,\mathcal{Z}_j^* + \mathcal{Z}_j\,\mathbf{i}\,\mathcal{Z}_{j-1}^*) + \alpha_{2,j}\,(\mathcal{Z}_{j-1}\,\mathbf{i}\,\mathcal{Z}_{j+1}^* + \mathcal{Z}_{j+1}\,\mathbf{i}\,\mathcal{Z}_{j-1}^*)\\
&\quad + \alpha_{3,j}\,(\mathcal{Z}_j\,\mathbf{i}\,\mathcal{Z}_j^*) + \alpha_{4,j}\,(\mathcal{Z}_j\,\mathbf{i}\,\mathcal{Z}_{j+1}^* + \mathcal{Z}_{j+1}\,\mathbf{i}\,\mathcal{Z}_j^*), \quad j=1,\dots,m-1,\\
\mathbf{p}_{3j} &= \beta_{1,j}\,(\mathcal{Z}_j\,\mathbf{i}\,\mathcal{Z}_j^*) + \beta_{2,j}\,(\mathcal{Z}_j\,\mathbf{i}\,\mathcal{Z}_{j+1}^* + \mathcal{Z}_{j+1}\,\mathbf{i}\,\mathcal{Z}_j^*), \quad j=0,\dots,m-1,\\
\mathbf{p}_{3j+1} &= \frac{1}{2}\beta_{1,j}\,(\mathcal{Z}_j\,\mathbf{i}\,\mathcal{Z}_{j+1}^* + \mathcal{Z}_{j+1}\,\mathbf{i}\,\mathcal{Z}_j^*) + 2\beta_{2,j}\,(\mathcal{Z}_{j+1}\,\mathbf{i}\,\mathcal{Z}_{j+1}^*), \quad j=0,\dots,m-1,
\end{aligned} \tag{6}$$

are the control points of the hodograph

$$\mathbf{p}(t) := \mathbf{r}'(t),$$

obtained by means of some quaternion coefficients $\mathcal{Z}_i$, $i=0,\dots,m$ and their conjugates $\mathcal{Z}_i^*$, and the real coefficients $\alpha_{l,j}$, $l=1,2,3,4$, $j=1,\dots,m-1$ in (1) and $\beta_{h,j}$, $h=1,2$, $j=0,\dots,m-1$ in (2).

Now, after introducing the abbreviations

(i) $\Delta_j := t_3 - t_2\,,\ j=0,\dots,4$ for the case $m=2$,

(ii) $\Delta_j := \begin{cases} t_3-t_2\,,\ j=0,1,2\\ t_4-t_2\,,\ j=3,4\\ t_4-t_3\,,\ j=5,6,7 \end{cases}$ for the case $m=3$,

(iii) $\Delta_j := \begin{cases} t_{3+\lfloor \frac{j}{3}\rfloor} - t_2\,,\ j=0,\dots,4\\ t_{3+\lfloor \frac{j}{3}\rfloor} - t_{1+\lfloor \frac{j+1}{3}\rfloor}\,,\ j=5,\dots,3m-7\\ t_{m+1} - t_{1+\lfloor \frac{j+1}{3}\rfloor}\,,\ j=3m-6,\dots,3m-2 \end{cases}$ for the case $m\geq 4$,

(where, for $x\in\mathbb{R}$, $\lfloor x\rfloor$ denotes the largest integer that is less than or equal to x), it is not difficult to observe that the control points of $\mathbf{r}(t)$ can be rewritten in the compact form

$$\mathbf{r}_i = \mathbf{r}_0 + \frac{1}{5}\sum_{j=0}^{i-1}\Delta_j\,\mathbf{p}_j\,, \quad i=1,\dots,3m-1.$$

In addition, exploiting the local support of the normalized quintic B–Splines $N^5_{i,\boldsymbol{\rho}}(t)$, $i=0,\dots,3m-1$, we can easily verify that for all $k=3,\dots,m$,

$$N^5_{i,\boldsymbol{\rho}}(t_k)\begin{cases} \neq 0\,, \text{ if } i=3k-6,3k-5,3k-4\\ =0\,, \text{ otherwise}\end{cases} \qquad \text{and} \qquad N^5_{3k-6,\boldsymbol{\rho}}(t_k) + N^5_{3k-5,\boldsymbol{\rho}}(t_k) + N^5_{3k-4,\boldsymbol{\rho}}(t_k) = 1\,.$$

Thanks to the last properties fulfilled by the control points and the basis functions of $\mathbf{r}(t)$, we can rewrite the equation system (3) as

$$\sum_{j=0}^{3k-5}\Gamma_{j,k}\,\mathbf{p}_j = \mathbf{c}_k - \mathbf{c}_2, \qquad k=2,\dots,m+1 \tag{7}$$

where

$$\begin{aligned}
\Gamma_{j,2} &:= 0, \quad j=0,1\\
\Gamma_{j,m+1} &:= \frac{\Delta_j}{5}, \quad j=0,\dots,3m-2,
\end{aligned}$$

and, for $k=3,\dots,m$,

$$\Gamma_{j,k} := \begin{cases} \dfrac{\Delta_j}{5}, & j=0,\dots,3k-7 \\ \dfrac{\Delta_j}{5}\left(N^5_{3k-5,\boldsymbol{\rho}}(t_k)+N^5_{3k-4,\boldsymbol{\rho}}(t_k)\right), & j=3k-6 \\ \dfrac{\Delta_j}{5}N^5_{3k-4,\boldsymbol{\rho}}(t_k), & j=3k-5. \end{cases}$$

As a consequence, starting from (7) we can easily write the $m-1$ equations

$$\sum_{j=0}^{3k-2}\Gamma_{j,k+1}\,\mathbf{p}_j-\sum_{j=0}^{3k-5}\Gamma_{j,k}\,\mathbf{p}_j=\mathbf{c}_{k+1}-\mathbf{c}_k,\qquad k=2,\dots,m,$$

and, exploiting the properties of $\Gamma_{j,k}$, obtain from the latter the equivalent $m-1$ conditions

$$\sum_{j=3k-6}^{3k-5}(\Gamma_{j,k+1}-\Gamma_{j,k})\,\mathbf{p}_j+\sum_{j=3k-4}^{3k-2}\Gamma_{j,k+1}\mathbf{p}_j=\mathbf{c}_{k+1}-\mathbf{c}_k\,,\qquad k=2,\dots,m. \tag{8}$$

The conditions in (8) provide a non-linear system made of $m-1$ vector valued equations in the $m+1$ quaternion unknowns $\mathcal{Z}_i$, $i=0,\dots,m$.
In the next subsection we introduce a computational approach that allows us to solve the interpolation problem described by the $m-1$ constraints in (8) by means of explicit formulas for computing $\mathcal{Z}_2,\dots,\mathcal{Z}_m$ in terms of the quaternions $\mathcal{Z}_0$, $\mathcal{Z}_1$ and the angular parameters $\phi_2,\dots,\phi_m\in[-\pi,\pi)$ paired with $\mathcal{Z}_2,\dots,\mathcal{Z}_m$, according to the relation later introduced in (11).

3.1 Towards explicit formulas solving the interpolation problem with C^2 clamped quintic PH B-spline curves

Due to the special dependency of the hodograph control points $\mathbf{p}_0,\dots,\mathbf{p}_{3m-2}$ in (6) on the unknown quaternions $\mathcal{Z}_i$, $i=0,\dots,m$, the equation system (8) allows an explicit solution. Indeed, by using (6), the equations in (8) may equivalently be rewritten as

$$\mathcal{A}\,\mathbf{i}\,\mathcal{A}^*=\Omega_k(\mathcal{Z}_{k-2},\mathcal{Z}_{k-1}),\qquad k=2,\dots,m \tag{9}$$

where

$$\mathcal{A}=\mathcal{Z}_k+\frac{\mathcal{G}_k(\mathcal{Z}_{k-2},\mathcal{Z}_{k-1})}{2\beta_{2,k-1}\Gamma_{3k-2,k+1}},$$

$$\Omega_k(\mathcal{Z}_{k-2},\mathcal{Z}_{k-1})=\frac{\mathcal{G}_k(\mathcal{Z}_{k-2},\mathcal{Z}_{k-1})\,\mathbf{i}\,\mathcal{G}_k(\mathcal{Z}_{k-2},\mathcal{Z}_{k-1})^*}{(2\beta_{2,k-1}\Gamma_{3k-2,k+1})^2}+\frac{\tilde{\Omega}_k(\mathcal{Z}_{k-2},\mathcal{Z}_{k-1})}{2\beta_{2,k-1}\Gamma_{3k-2,k+1}},$$

and

$$\mathcal{G}_k(\mathcal{Z}_{k-2},\mathcal{Z}_{k-1})\;=\Gamma_{3k-4,k+1}\,\alpha_{2,k-1}\,\mathcal{Z}_{k-2}+\left(\Gamma_{3k-4,k+1}\,\alpha_{4,k-1}+\Gamma_{3k-3,k+1}\,\beta_{2,k-1}+\Gamma_{3k-2,k+1}\,\tfrac{\beta_{1,k-1}}{2}\right)\mathcal{Z}_{k-1}\,,$$

with

$$\begin{aligned}\tilde{\Omega}_k(\mathcal{Z}_{k-2},\mathcal{Z}_{k-1})\;&=\mathbf{c}_{k+1}-\mathbf{c}_k-(\Gamma_{3k-6,k+1}-\Gamma_{3k-6,k})\Big[\beta_{1,k-2}\,(\mathcal{Z}_{k-2}\,\mathbf{i}\,\mathcal{Z}^*_{k-2})+\beta_{2,k-2}\,(\mathcal{Z}_{k-2}\,\mathbf{i}\,\mathcal{Z}^*_{k-1}+\mathcal{Z}_{k-1}\,\mathbf{i}\,\mathcal{Z}^*_{k-2})\Big]\\&\quad-(\Gamma_{3k-5,k+1}-\Gamma_{3k-5,k})\Big[\tfrac{\beta_{1,k-2}}{2}\,(\mathcal{Z}_{k-2}\,\mathbf{i}\,\mathcal{Z}^*_{k-1}+\mathcal{Z}_{k-1}\,\mathbf{i}\,\mathcal{Z}^*_{k-2})+2\beta_{2,k-2}\,(\mathcal{Z}_{k-1}\,\mathbf{i}\,\mathcal{Z}^*_{k-1})\Big]\\&\quad-\Gamma_{3k-4,k+1}\Big[\alpha_{1,k-1}\,(\mathcal{Z}_{k-2}\,\mathbf{i}\,\mathcal{Z}^*_{k-1}+\mathcal{Z}_{k-1}\,\mathbf{i}\,\mathcal{Z}^*_{k-2})+\alpha_{3,k-1}\,(\mathcal{Z}_{k-1}\,\mathbf{i}\,\mathcal{Z}^*_{k-1})\Big]-\Gamma_{3k-3,k+1}\,\beta_{1,k-1}\,\mathcal{Z}_{k-1}\,\mathbf{i}\,\mathcal{Z}^*_{k-1}\,,\end{aligned}$$

and $\alpha_{r,l}$, $r=1,2,3,4$, $l=1,\dots,m-1$ as in (1) and $\beta_{h,l}$, $h=1,2$, $l=0,\dots,m-1$ as in (2).

We now introduce the following auxiliary result, previously given in many other papers (see, e.g., [2, Lemma 4.1], [8, Section 3.2] or [10, Section 2.1]), that allows us to solve (9) explicitly.

Lemma 3.1. *Let* $\mathbf{c}$ *be a given pure vector quaternion. All the solutions of the equation*

$$\mathcal{A}\,\mathbf{i}\,\mathcal{A}^*=\mathbf{c} \tag{10}$$

form a one-parameter family

$$\mathcal{A}(\mathbf{c},\phi)=\mathcal{A}_p(\mathbf{c})\mathcal{Q}_\phi\,,$$

where $\mathcal{Q}_\phi=\cos(\phi)+\mathbf{i}\sin(\phi)$ *with* $\phi\in[-\pi,\pi)$*, and*

$$\mathcal{A}_p(\mathbf{c})=\begin{cases}\sqrt{|\mathbf{c}|}\,\dfrac{\frac{\mathbf{c}}{|\mathbf{c}|}+\mathbf{i}}{\left|\frac{\mathbf{c}}{|\mathbf{c}|}+\mathbf{i}\right|}, & \text{if } \frac{\mathbf{c}}{|\mathbf{c}|}\neq-\mathbf{i}\\ \sqrt{|\mathbf{c}|}\,\mathbf{k}\,, & \text{if } \frac{\mathbf{c}}{|\mathbf{c}|}=-\mathbf{i}\end{cases}$$

is a particular solution of (10).

Indeed, by applying Lemma 3.1 to equation (9), we obtain for the quaternion $\mathcal{Z}_k$ the explicit expression

$$\mathcal{Z}_k = -\frac{\mathcal{G}_k(\mathcal{Z}_{k-2}, \mathcal{Z}_{k-1})}{2\beta_{2,k-1}\Gamma_{3k-2,k+1}} + \mathcal{A}(\Omega_k(\mathcal{Z}_{k-2}, \mathcal{Z}_{k-1}), \phi_k), \qquad k = 2, \ldots, m \tag{11}$$

with $\phi_k \in [-\pi, \pi)$ denoting the angular parameter that allows us to incorporate all possible solutions to equation (9).

To summarize, the interpolation method for open sequences of 3D-data consists in arbitrarily choosing $\mathcal{Z}_0, \mathcal{Z}_1, \phi_2, \ldots, \phi_m$ (which correspond to $m+7$ scalar free parameters) and determining the remaining unknowns $\mathcal{Z}_2, \ldots, \mathcal{Z}_m$ from them by using (11). In practice, since there are $m+7$ scalar free parameters, we can construct more than one interpolant for each considered data set $\mathbf{c}_k$, $k = 2, \ldots, m+1$. The resulting C^2 quintic PH interpolants will be different because, even if they share the same degree 5 and the same knot partition $\boldsymbol{\rho}$, they differ in the arrangement of the control points $\mathbf{r}_0, \ldots, \mathbf{r}_{3m-1}$ which depend on the free parameters $\mathcal{Z}_0, \mathcal{Z}_1, \phi_2, \ldots, \phi_m$, thus providing different shapes. In Section 5.1 we will describe the proposed interpolation method in algorithmic form, pointing out a possible strategy to select the free parameters.

4 Formulating the interpolation problem for closed sequences of 3D-data

For a given sequence of $m+2$ 3D-points $\mathbf{c}_k$, $k = 2, \ldots, m+3$ where $m \geq 2$ and $\mathbf{c}_{m+3} = \mathbf{c}_2$, the problem we would like to investigate consists in designing a numerical procedure to determine a C^2 periodic quintic PH B-spline curve

$$\mathbf{r} : [0, 1] \to \mathbb{R}^3$$

that satisfies the closure conditions

$$\mathbf{r}(0) = \mathbf{r}(1), \quad \mathbf{r}'(0) = \mathbf{r}'(1), \quad \mathbf{r}''(0) = \mathbf{r}''(1) \tag{12}$$

and the interpolation conditions

$$\mathbf{r}(t_k) = \mathbf{c}_k, \quad k = 2, \ldots, m+3. \tag{13}$$

As in the previous section, the knots t_k, $k = 2, \ldots, m+3$ can be computed by standard parametrization techniques, with the only precaution of enforcing the periodicity of the knot partition that is required to achieve a C^2 closure of the PH B-spline curve. This means that, after computing

$$\tau_0 = 0, \qquad \tau_i = \tau_{i-1} + \|\mathbf{c}_{i+2} - \mathbf{c}_{i+1}\|_2^{\theta}, \quad i = 1, \ldots, m+1 \quad \text{with} \quad \theta \in \left\{0, \frac{1}{2}, 1\right\},$$

we shall set

$$t_k := \frac{\tau_{k-2}}{\tau_{m+1}}, \; k = 2, \ldots, m+3 \qquad \text{and assume} \qquad t_1 := t_2 - (t_{m+3} - t_{m+2}), \quad t_{m+4} := t_{m+3} + (t_3 - t_2). \tag{14}$$

The definition of the periodic knot partition $\boldsymbol{\rho}$ of $\mathbf{r}(t)$ must then be completed by introducing the additional knots t_{-1}, t_0 and t_{m+5}, t_{m+6} that may assume any arbitrary location complying with the ascending ordering of the resulting knot vector

$$\boldsymbol{\rho} := \left\{t_{-1}, \{\langle t_k \rangle^3\}_{k=0,\ldots,m+5}, t_{m+6}\right\}.$$

The knot intervals associated with $\boldsymbol{\rho}$ are defined as

$$d_i := t_i - t_{i-1}, \quad i = 1, \ldots, m+5$$

and fulfill the periodicity constraints

$$d_{m+3} = d_2 \quad \text{and} \quad d_{m+4} = d_3 \tag{15}$$

implied by (14). As to the control points of the C^2 periodic quintic PH B-spline curve

$$\mathbf{r}(t) = \sum_{i=0}^{3m+13} \mathbf{r}_i N_{i,\boldsymbol{\rho}}^5(t), \quad t \in [0, 1], \tag{16}$$

recalling the results in [2, Section 3.2.2] we assume them to satisfy the relations

$$\begin{aligned}
&\mathbf{r}_2 = \mathbf{r}_1 = \mathbf{r}_0, \\
&\mathbf{r}_3 = \mathbf{r}_2 + \frac{d_1}{5}\mathcal{Z}_0\,\mathbf{i}\,\mathcal{Z}_0^*, \\
&\mathbf{r}_{3j+1} = \mathbf{r}_{3j} + \frac{d_{j+1}}{5}\mathbf{p}_{3j}, \quad j = 1, \ldots, m+3, \\
&\mathbf{r}_{3j+2} = \mathbf{r}_{3j+1} + \frac{d_{j+1} + d_{j+2}}{5}\mathbf{p}_{3j+1}, \quad j = 1, \ldots, m+2, \\
&\mathbf{r}_{3j+3} = \mathbf{r}_{3j+2} + \frac{d_{j+1} + d_{j+2}}{5}\mathbf{p}_{3j+2}, \quad j = 1, \ldots, m+2, \\
&\mathbf{r}_{3m+11} = \mathbf{r}_{3m+10} + \frac{d_{m+5}}{5}\mathcal{Z}_{m+2}\,\mathbf{i}\,\mathcal{Z}_{m+2}^*, \\
&\mathbf{r}_{3m+13} = \mathbf{r}_{3m+12} = \mathbf{r}_{3m+11},
\end{aligned} \tag{17}$$

where $\mathbf{r}_0$ is an arbitrary 3D-point and

$$\begin{aligned}
\mathbf{p}_{3j-3} &= \alpha_{1,j}\,(\mathcal{Z}_{j-3}\,\mathbf{i}\,\mathcal{Z}^*_{j-2}+\mathcal{Z}_{j-2}\,\mathbf{i}\,\mathcal{Z}^*_{j-3})+\alpha_{2,j}\,(\mathcal{Z}_{j-3}\,\mathbf{i}\,\mathcal{Z}^*_{j-1}+\mathcal{Z}_{j-1}\,\mathbf{i}\,\mathcal{Z}^*_{j-3})\\
&\quad +\alpha_{3,j}\,(\mathcal{Z}_{j-2}\,\mathbf{i}\,\mathcal{Z}^*_{j-2})+\alpha_{4,j}\,(\mathcal{Z}_{j-2}\,\mathbf{i}\,\mathcal{Z}^*_{j-1}+\mathcal{Z}_{j-1}\,\mathbf{i}\,\mathcal{Z}^*_{j-2}),\quad j=1,\dots,m+5,\\
\mathbf{p}_{3j-2} &= \beta_{1,j}\,(\mathcal{Z}_{j-2}\,\mathbf{i}\,\mathcal{Z}^*_{j-2})+\beta_{2,j}\,(\mathcal{Z}_{j-2}\,\mathbf{i}\,\mathcal{Z}^*_{j-1}+\mathcal{Z}_{j-1}\,\mathbf{i}\,\mathcal{Z}^*_{j-2}),\quad j=1,\dots,m+4,\\
\mathbf{p}_{3j-1} &= \frac{\beta_{1,j}}{2}\,(\mathcal{Z}_{j-2}\,\mathbf{i}\,\mathcal{Z}^*_{j-1}+\mathcal{Z}_{j-1}\,\mathbf{i}\,\mathcal{Z}^*_{j-2})+2\,\beta_{2,j}\,(\mathcal{Z}_{j-1}\,\mathbf{i}\,\mathcal{Z}^*_{j-1}),\quad j=1,\dots,m+4,
\end{aligned}\tag{18}$$

are the control points of the hodograph

$$\mathbf{p}(t) := \mathbf{r}'(t),$$

obtained by means of the quaternion coefficients $\mathcal{Z}_{-2}=\mathcal{Z}_{-1}=\mathcal{Z}_{m+3}=\mathcal{Z}_{m+4}=\mathbf{0}$, some unknown quaternion coefficients $\mathcal{Z}_i$, $i=0,\dots,m+2$ and their conjugates, as well as the real coefficients $\alpha_{l,j}$, $l=1,2,3,4$, $j=1,\dots,m+5$ in (1) and $\beta_{h,j}$, $h=1,2$, $j=1,\dots,m+4$ in (2). Note that, in practice, it is not needed to know the coefficients $\alpha_{l,1}$, $l=1,2,3,4$ explicitly since the expressions they multiply are all zero pure vector quaternions.

As in the clamped case, we then proceed by introducing the abbreviations

$$\Delta_i := t_{\lfloor\frac{i+5}{3}\rfloor}-t_{\lfloor\frac{i}{3}\rfloor},\quad i=0,\dots,3m+12$$

that allow us to rewrite the control points of $\mathbf{r}(t)$ in the compact form

$$\mathbf{r}_i=\mathbf{r}_0+\frac{1}{5}\sum_{j=0}^{i-1}\Delta_j\mathbf{p}_j,\qquad i=1,\dots,3m+13.$$

In addition, exploiting the local support of the normalized quintic B–Splines $N^5_{i,\boldsymbol{\rho}}(t)$, $i=0,\dots,3m+13$ we observe that, for $k=2,\dots,m+3$,

$$N^5_{i,\boldsymbol{\rho}}(t_k)\begin{cases}\neq 0, \text{ if } i=3k-2,3k-1,3k\\ =0, \text{ otherwise}\end{cases}\qquad\text{and}\qquad N^5_{3k-2,\boldsymbol{\rho}}(t_k)+N^5_{3k-1,\boldsymbol{\rho}}(t_k)+N^5_{3k,\boldsymbol{\rho}}(t_k)=1.$$

The equation system (13) can thus be equivalently rewritten as

$$\sum_{j=0}^{3k-1}\Gamma_{j,k}\mathbf{p}_j=\mathbf{c}_k-\mathbf{r}_0,\qquad k=2,\dots,m+3\tag{19}$$

with

$$\Gamma_{j,k}=\begin{cases}\dfrac{\Delta_j}{5}, & j=0,\dots,3k-3\\[2mm] \dfrac{\Delta_j}{5}\left(N^5_{3k-1,\boldsymbol{\rho}}(t_k)+N^5_{3k,\boldsymbol{\rho}}(t_k)\right), & j=3k-2\\[2mm] \dfrac{\Delta_j}{5}N^5_{3k,\boldsymbol{\rho}}(t_k), & j=3k-1.\end{cases}$$

Starting from (19) we can thus rewrite the equation system yielding the interpolation constraints in the equivalent form

$$\begin{cases}\displaystyle\sum_{j=0}^{5}\Gamma_{j,2}\mathbf{p}_j &= \mathbf{c}_2-\mathbf{r}_0,\\ \displaystyle\sum_{j=3k-2}^{3k-1}(\Gamma_{j,k+1}-\Gamma_{j,k})\,\mathbf{p}_j+\sum_{j=3k}^{3k+2}\Gamma_{j,k+1}\mathbf{p}_j &= \mathbf{c}_{k+1}-\mathbf{c}_k,\quad k=2,\dots,m+2.\end{cases}\tag{20}$$

Note that, the equation system (20) amounts to $m+2$ vector valued equations. Since the next three additional conditions

$$\sum_{j=6}^{3m+8}\Delta_j\,\mathbf{p}_j=\sum_{j=5}^{3m+7}\Delta_j\,\mathbf{p}_j=\sum_{j=4}^{3m+6}\Delta_j\,\mathbf{p}_j=\mathbf{0}\tag{21}$$

must be taken into account to guarantee the closure of the curve $\mathbf{r}(t)$ as specified in (12), all together (20) and (21) provide $m+5$ vector valued equations for $m+3$ quaternion unknowns $\mathcal{Z}_i$, $i=0,\dots,m+2$, which amount to $m-3$ scalar free parameters. Moreover, three additional degrees of freedom are provided by the 3D coordinates of the arbitrary point $\mathbf{r}_0$. Therefore the overall number of degrees of freedom turns out to be m. In the following subsection we introduce a computational approach that allows us: (i) to solve the last $m+1$ vector valued equations in (20) by means of explicit formulas for computing $\mathcal{Z}_2,\dots,\mathcal{Z}_{m+2}$ in terms of the quaternions $\mathcal{Z}_0,\mathcal{Z}_1$ and the angular parameters $\phi_2,\dots,\phi_{m+2}$; (ii) to obtain from the first equation in (20) the expression of $\mathbf{r}_0$ in terms of the quaternions $\mathcal{Z}_0$, $\mathcal{Z}_1$ and their conjugates. Since the conditions in (21) are made of 9 scalar equations in the previous unknowns (i.e., $\mathcal{Z}_0$, $\mathcal{Z}_1$, $\phi_2,\dots,\phi_{m+2}$), the degrees of freedom decrease from $m+9$ to m scalars.

4.1 Towards explicit formulas solving the interpolation problem with C^2 periodic quintic PH B-spline curves

We start from observing that the first equation in (20) is equivalent to

$$\mathbf{r}_0 = \mathbf{c}_2 - (2\beta_{2,1}\Gamma_{2,2} + \alpha_{3,2}\Gamma_{3,2} + \beta_{1,2}\Gamma_{4,2})(\mathcal{Z}_0\,\mathbf{i}\,\mathcal{Z}_0^*) - \left(\alpha_{4,2}\Gamma_{3,2} + \beta_{2,2}\Gamma_{4,2} + \frac{\beta_{1,2}}{2}\Gamma_{5,2}\right)(\mathcal{Z}_0\,\mathbf{i}\,\mathcal{Z}_1^* + \mathcal{Z}_1\,\mathbf{i}\,\mathcal{Z}_0^*) - 2\beta_{2,2}\Gamma_{5,2}(\mathcal{Z}_1\,\mathbf{i}\,\mathcal{Z}_1^*), \quad (22)$$

whereas the remaining equations can be rewritten as

$$\mathcal{A}\,\mathbf{i}\,\mathcal{A}^* = \Omega_k(\mathcal{Z}_{k-2}, \mathcal{Z}_{k-1}), \quad k = 2, \ldots, m+2, \quad (23)$$

where

$$\mathcal{A} = \mathcal{Z}_k + \frac{1}{2\,\beta_{2,k+1}\,\Gamma_{3k+2,k+1}}\mathcal{G}_k(\mathcal{Z}_{k-2}, \mathcal{Z}_{k-1}),$$

$$\Omega_k(\mathcal{Z}_{k-2}, \mathcal{Z}_{k-1}) = \frac{\mathcal{G}_k(\mathcal{Z}_{k-2}, \mathcal{Z}_{k-1})\,\mathbf{i}\,\mathcal{G}_k(\mathcal{Z}_{k-2}, \mathcal{Z}_{k-1})^*}{(2\,\beta_{2,k+1}\,\Gamma_{3k+2,k+1})^2} + \frac{\tilde{\Omega}_k(\mathcal{Z}_{k-2}, \mathcal{Z}_{k-1})}{2\,\beta_{2,k+1}\,\Gamma_{3k+2,k+1}},$$

$$\mathcal{G}_k(\mathcal{Z}_{k-2}, \mathcal{Z}_{k-1}) = \Gamma_{3k,k+1}\,\alpha_{2,k+1}\mathcal{Z}_{k-2} + \left(\Gamma_{3k,k+1}\,\alpha_{4,k+1} + \Gamma_{3k+1,k+1}\,\beta_{2,k+1} + \Gamma_{3k+2,k+1}\,\frac{\beta_{1,k+1}}{2}\right)\mathcal{Z}_{k-1},$$

with

$$\begin{aligned}\tilde{\Omega}_k(\mathcal{Z}_{k-2}, \mathcal{Z}_{k-1}) \quad &= \mathbf{c}_{k+1} - \mathbf{c}_k - (\Gamma_{3k-2,k+1} - \Gamma_{3k-2,k})\Big[\beta_{1,k}\,(\mathcal{Z}_{k-2}\,\mathbf{i}\,\mathcal{Z}_{k-2}^*) + \beta_{2,k}\,(\mathcal{Z}_{k-2}\,\mathbf{i}\,\mathcal{Z}_{k-1}^* + \mathcal{Z}_{k-1}\,\mathbf{i}\,\mathcal{Z}_{k-2}^*)\Big]\\ &-(\Gamma_{3k-1,k+1} - \Gamma_{3k-1,k})\Big[\tfrac{\beta_{1,k}}{2}\,(\mathcal{Z}_{k-2}\,\mathbf{i}\,\mathcal{Z}_{k-1}^* + \mathcal{Z}_{k-1}\,\mathbf{i}\,\mathcal{Z}_{k-2}^*) + 2\beta_{2,k}\,(\mathcal{Z}_{k-1}\,\mathbf{i}\,\mathcal{Z}_{k-1}^*)\Big]\\ &-\Gamma_{3k,k+1}\Big[\alpha_{1,k+1}\,(\mathcal{Z}_{k-2}\,\mathbf{i}\,\mathcal{Z}_{k-1}^* + \mathcal{Z}_{k-1}\,\mathbf{i}\,\mathcal{Z}_{k-2}^*) + \alpha_{3,k+1}\,(\mathcal{Z}_{k-1}\,\mathbf{i}\,\mathcal{Z}_{k-1}^*)\Big] - \Gamma_{3k+1,k+1}\,\beta_{1,k+1}\,(\mathcal{Z}_{k-1}\,\mathbf{i}\,\mathcal{Z}_{k-1}^*),\end{aligned}$$

and $\alpha_{h,l}$, $\beta_{h,l}$ as in (1), (2) respectively.
By applying Lemma 3.1, equation (23) can be solved so obtaining the explicit solution

$$\mathcal{Z}_k \quad = \quad -\frac{\mathcal{G}_k(\mathcal{Z}_{k-2}, \mathcal{Z}_{k-1})}{2\,\beta_{2,k+1}\,\Gamma_{3k+2,k+1}} + \mathcal{A}\Big(\Omega_k(\mathcal{Z}_{k-2}, \mathcal{Z}_{k-1}), \phi_k\Big), \quad k = 2, \ldots, m+2, \quad (24)$$

with $\phi_k \in [-\pi, \pi)$ denoting the angular parameter that allows us to incorporate all possible solutions to (23).

Replacing the previously calculated quaternions $\mathcal{Z}_2, \ldots, \mathcal{Z}_{m+2}$ into the expressions of the $\mathbf{p}_j$ control points that appear in the three vector valued equations (21) yields a nonlinear system of 9 scalar equations in the $m+9$ unknowns $\mathcal{Z}_0$, $\mathcal{Z}_1$, $\phi_2, \ldots, \phi_{m+2}$ that, to be satisfied, reduces the degrees of freedom to m scalars. An algorithmic formulation of the proposed interpolation method is given in Section 5.2.

5 The interpolation method in algorithmic form

To facilitate reproduction of the interpolation method proposed in this paper, we here describe the numerical procedure that can be used to construct either a C^2 clamped quintic PH B-spline curve that interpolates an open dataset $\{\mathbf{c}_k,\ k = 2, \ldots, m+1\}$, or a C^2 periodic quintic PH B-spline curve that interpolates a closed dataset $\{\mathbf{c}_k,\ k = 2, \ldots, m+3\}$ with $\mathbf{c}_{m+3} = \mathbf{c}_2$.

5.1 Numerical procedure to interpolate an open dataset

Input: the sequence of 3D-points $\{\mathbf{c}_k,\ k = 2, \ldots, m+1\}$;
the value of $\theta \in \left\{0, \frac{1}{2}, 1\right\}$ to be used to compute the knots $\{t_k,\ k = 2, \ldots, m+1\}$;
suitable initial angles $\phi_2^p, \ldots, \phi_m^p \in [-\pi, \pi)$ and initial quaternions $\mathcal{Z}_0^p$, $\mathcal{Z}_1^p$.

The interpolation algorithm (for open datasets):

O1. Construct the C^2 clamped quintic PH B-spline curve $\mathbf{r}(t)$, $t \in [0, 1]$ whose control points $\mathbf{r}_0, \ldots, \mathbf{r}_{3m-1}$ (depending on $\mathcal{Z}_0$, $\mathcal{Z}_1$, $\phi_2, \ldots, \phi_m$) are such that the energy measure

$$\hat{E}_1(\mathcal{Z}_0, \mathcal{Z}_1, \phi_2, \ldots, \phi_m) = G(\mathcal{Z}_0, \mathcal{Z}_1, \phi_2, \ldots, \phi_m)\; E_1(\mathcal{Z}_0, \mathcal{Z}_1, \phi_2, \ldots, \phi_m) \quad (25)$$

with

$$G(\mathcal{Z}_0, \mathcal{Z}_1, \phi_2, \ldots, \phi_m) = \int_0^1 |\mathbf{r}'(t)|\; dt\,,$$

$$E_1(\mathcal{Z}_0, \mathcal{Z}_1, \phi_2, \ldots, \phi_m) = \int_0^1 \kappa^2(t)\; |\mathbf{r}'(t)|\; dt$$

and $\kappa(t)$ the curvature of $\mathbf{r}(t)$, is minimized. Here the functional $\hat{E}_1$ is a scale-invariant version of the curvature-based energy functional E_1 (see [2] and references therein).
Performing this minimization with Matlab standard solver `fmincon` relying on the interior-point algorithm, starting at $\mathcal{Z}_0^p$, $\mathcal{Z}_1^p$, $\phi_2^p, \ldots, \phi_m^p$ and setting lower bounds $-\pi$ and upper bounds π on the angular values, yields new values $\phi_2^f, \ldots, \phi_m^f$ (that fulfill the required constraints $-\pi \le \phi_j^f < \pi$, for all $j = 2, \ldots, m$) and new quaternions $\mathcal{Z}_0^f$, $\mathcal{Z}_1^f$.

O2. Exploit the quaternions $\mathcal{Z}_0^f, \mathcal{Z}_1^f$ and the angular values $\phi_2^f, \dots, \phi_m^f$ obtained in step [O1.] to compute the quaternions $\mathcal{Z}_2^f, \dots, \mathcal{Z}_m^f$ from (11).

O3. Determine the control points $\mathbf{r}_1, \dots, \mathbf{r}_{3m-1}$ of $\mathbf{r}(t)$ from $\mathbf{r}_0 = \mathbf{c}_2$ and the above $\mathcal{Z}_j^f$, $j = 0, \dots, m$ by means of (5) and (6).

Output: $\mathbf{r}(t)$ in (4) that satisfies (3).

5.2 Numerical procedure to interpolate a closed dataset

Input: the sequence of 3D-points $\{\mathbf{c}_k,\ k = 2, \dots, m+3\}$ with $\mathbf{c}_{m+3} = \mathbf{c}_2$;
the value of $\theta \in \left\{0, \frac{1}{2}, 1\right\}$ to be used to compute the knots $\{t_k,\ k = 2, \dots, m+3\}$;
suitable initial angles $\phi_2^p, \dots, \phi_{m+2}^p \in [-\pi, \pi)$ and initial quaternions $\mathcal{Z}_0^p$, $\mathcal{Z}_1^p$.

The interpolation algorithm (for closed datasets):

C1. Construct the C^2 periodic quintic PH B-spline curve $\mathbf{r}(t)$, $t \in [0,1]$ whose control points $\mathbf{r}_0, \dots, \mathbf{r}_{3m+13}$ (depending on $\mathcal{Z}_0$, $\mathcal{Z}_1$, $\phi_2, \dots, \phi_{m+2}$) are such that the scale-invariant energy measure $\hat{E}_1(\mathcal{Z}_0, \mathcal{Z}_1, \phi_2, \dots, \phi_{m+2}) = \left(\int_0^1 |\mathbf{r}'(t)|\, dt\right)\left(\int_0^1 \kappa^2(t)\, |\mathbf{r}'(t)|\, dt\right)$ is minimized and, at the same time, the conditions in (21) are satisfied. Performing this constrained minimization with Matlab standard solver `fmincon` relying on the interior-point algorithm, starting at $\mathcal{Z}_0^p, \mathcal{Z}_1^p$, $\phi_2^p, \dots, \phi_{m+2}^p$ and setting suitable lower and upper bounds on the angular values, yields new values $\phi_2^f, \dots, \phi_{m+2}^f$ (that fulfill the required constraints) and new quaternions $\mathcal{Z}_0^f, \mathcal{Z}_1^f$.

C2. Exploit the quaternions $\mathcal{Z}_0^f, \mathcal{Z}_1^f$ and the angular values $\phi_2^f, \dots, \phi_{m+2}^f$ obtained in step [C1.] to compute the quaternions $\mathcal{Z}_2^f, \dots, \mathcal{Z}_{m+2}^f$ from (24).

C3. Compute the control point $\mathbf{r}_0$ through (22).

C4. Determine the control points $\mathbf{r}_1, \dots, \mathbf{r}_{3m+13}$ of $\mathbf{r}(t)$ from $\mathbf{r}_0$ and the above $\mathcal{Z}_j^f$, $j = 0, \dots, m+2$ by means of (17) and (18).

Output: $\mathbf{r}(t)$ in (16) that satisfies (13).

6 Numerical examples

In the following we provide examples of open and closed C^2 quintic PH B-spline interpolants obtained through the proposed numerical procedures by choosing $\theta = 1$ in the construction of the knot partition. For both open and closed curves, such procedures rely on minimization algorithms that need to start from a suitable initial guess (consisting of the angular values and the two quaternions required as input by the numerical procedures) in order to converge to a good curve.

As to open curves, the initial guess consists of the angles $\phi_2^p, \dots, \phi_m^p$ and the quaternions $\mathcal{Z}_0^p$, $\mathcal{Z}_1^p$, and it may be easily obtained through the following preprocessing strategy.

Open curves preprocessing phase: Choose values $\phi_2^i, \dots, \phi_m^i$ randomly in $(0,1) \subset [-\pi, \pi)$, as well as quaternions $\mathcal{Z}_0^i$, $\mathcal{Z}_1^i$ with all entries randomly selected in $(0,1)$. Then construct the C^2 clamped quintic PH B-spline curve $\mathbf{r}(t)$, $t \in [0,1]$ whose control points $\mathbf{r}_0, \dots, \mathbf{r}_{3m-1}$ (depending on $\mathcal{Z}_0$, $\mathcal{Z}_1$, $\phi_2, \dots, \phi_m$) are such that its total arc length

$$G(\mathcal{Z}_0, \mathcal{Z}_1, \phi_2, \dots, \phi_m) = \int_0^1 |\mathbf{r}'(t)|\, dt$$

is minimized. Performing this minimization with Matlab standard solver `fmincon` relying on the interior-point algorithm, starting at $\mathcal{Z}_0^i, \mathcal{Z}_1^i$, $\phi_2^i, \dots, \phi_m^i$ and setting lower bounds $-\pi$ and upper bounds π on the angular values, yields new values $\phi_2^p, \dots, \phi_m^p$ (that fulfill the required constraints $-\pi \le \phi_j^p < \pi$, for all $j = 2, \dots, m$) and new quaternions $\mathcal{Z}_0^p, \mathcal{Z}_1^p$. All together, the obtained values $\phi_2^p, \dots, \phi_m^p$ and the quaternions $\mathcal{Z}_0^p, \mathcal{Z}_1^p$ identify the additional input data required by the procedure in Subsection 5.1.

The first example in Figure 1 (first row) is a C^2 clamped quintic PH B-spline curve with $m = 5$, which interpolates 5 points on the parametric curve $(u^3 - 3u,\ u^4 - 4u^2,\ \frac{1}{5}u^5 - 2u)$, that are sampled at equispaced values $u \in [-2, 2]$. For this curve, the initial parameters computed randomly (that we passed to the preprocessing strategy), are

$$\phi_2^i = 0.6538, \quad \phi_3^i = 0.4942, \quad \phi_4^i = 0.7791, \quad \phi_5^i = 0.7150,$$
$$\mathcal{Z}_0^i = (0.9037, 0.8909, 0.3342, 0.6987)^T, \quad \mathcal{Z}_1^i = (0.1978, 0.0305, 0.7441, 0.5000)^T.$$

The input values of the procedure in Subsection 5.1, obtained as output of the preprocessing phase, are

$$\phi_2^p = 1.3382, \quad \phi_3^p = -2.3761, \quad \phi_4^p = 2.2953, \quad \phi_5^p = -0.0383,$$
$$\mathcal{Z}_0^p = (1.9196, 8.5237, -3.3949, 4.1183)^T, \quad \mathcal{Z}_1^p = (-6.5680, 0.1124, 2.6756, -1.6032)^T,$$

and the final ones (obtained at the end of step [O1.]) are

$$\phi_2^f = -0.7801, \quad \phi_3^f = -2.1033, \quad \phi_4^f = 2.4824, \quad \phi_5^f = 1.1088,$$
$$\mathcal{Z}_0^f = (-1.9230, 5.5580, -3.8992, 1.8171)^T, \quad \mathcal{Z}_1^f = (3.3575, 4.4659, -1.5323, 0.4319)^T.$$

The second example in Figure 1 (second row) is a C^2 clamped quintic PH B-spline curve with $m = 6$, which interpolates the 6 3D-points

$$\mathbf{c}_2 = (0,0,0)^T, \quad \mathbf{c}_3 = (-5,5,2)^T, \quad \mathbf{c}_4 = (0,10,-2)^T,$$
$$\mathbf{c}_5 = (8,12,5)^T, \quad \mathbf{c}_6 = (15,2,3)^T, \quad \mathbf{c}_7 = (2,0,7)^T,$$

suggested in [13, page 18]. For this curve, the initial parameters computed randomly (that we passed to the preprocessing strategy), are

$$\phi_2^i = 0.4854, \quad \phi_3^i = 0.8003, \quad \phi_4^i = 0.1419, \quad \phi_5^i = 0.4218, \quad \phi_6^i = 0.9157,$$
$$\mathcal{Z}_0^i = (0.7922, 0.9595, 0.6557, 0.0357)^T, \quad \mathcal{Z}_1^i = (0.8491, 0.9340, 0.6787, 0.7577)^T.$$

The input values of the procedure in Subsection 5.1, obtained as output of the preprocessing phase, are

$$\phi_2^p = 0.2933, \quad \phi_3^p = 1.0874, \quad \phi_4^p = 1.0447, \quad \phi_5^p = 1.3115, \quad \phi_6^p = 0.2528,$$
$$\mathcal{Z}_0^p = (-1.3329, -0.4972, 9.4586, 6.7601)^T, \quad \mathcal{Z}_1^p = (1.2997, 6.4714, 6.8938, 0.6817)^T,$$

and the final ones (obtained at the end of step [O1.]) are

$$\phi_2^f = 0.1263, \quad \phi_3^f = 0.8417, \quad \phi_4^f = 0.2402, \quad \phi_5^f = -0.2202, \quad \phi_6^f = -0.0106,$$
$$\mathcal{Z}_0^f = (-0.6005, 6.2744, 11.5077, 4.9314)^T, \quad \mathcal{Z}_1^f = (3.0989, -0.7824, 2.3348, 4.6042)^T.$$

Finally, the third example in Figure 1 (third row) is a C^2 clamped quintic PH B-spline curve with $m = 7$, which interpolates 7 points on the parametric curve $(\sin(u^2), u+1, u^2)$, that are sampled at equispaced values $u \in [-\pi/2, \pi/2]$. For this curve, the initial parameters computed randomly (that we passed to the preprocessing strategy), are

$$\phi_2^i = 0.7303, \quad \phi_3^i = 0.4886, \quad \phi_4^i = 0.5785, \quad \phi_5^i = 0.2373, \quad \phi_6^i = 0.4588, \quad \phi_7^i = 0.9631,$$
$$\mathcal{Z}_0^i = (0.5468, 0.5211, 0.2316, 0.4889)^T, \quad \mathcal{Z}_1^i = (0.6241, 0.6791, 0.3955, 0.3674)^T.$$

The input values of the procedure in Subsection 5.1, obtained as output of the preprocessing phase, are

$$\phi_2^p = -0.3958, \quad \phi_3^p = -0.9118, \quad \phi_4^p = -0.1919, \quad \phi_5^p = 0.8736, \quad \phi_6^p = 0.8584, \quad \phi_7^p = -0.0012,$$
$$\mathcal{Z}_0^p = (1.9676, 2.3627, 2.4951, -1.3092)^T, \quad \mathcal{Z}_1^p = (0.0338, 1.6733, -0.3173, -1.0902)^T,$$

and the final ones (obtained at the end of step [O1.]) are

$$\phi_2^f = -0.5630, \quad \phi_3^f = -0.6304, \quad \phi_4^f = -0.5852, \quad \phi_5^f = -0.0587, \quad \phi_6^f = 0.5789, \quad \phi_7^f = 0.3649,$$
$$\mathcal{Z}_0^f = (1.1923, 1.5263, 1.0841, -0.7014)^T, \quad \mathcal{Z}_1^f = (1.3455, 2.0061, 1.2491, -0.9463)^T.$$

For all the open curve examples we have tested, we have observed that, if the polygon connecting the interpolation points presents any symmetries, then such symmetries are preserved in the interpolating PH curve. This symmetry-preservation property is illustrated in the first and last row of Figure 1 and can be appreciated both looking at the curves shape and at their curvature plots.

We finally emphasize that the preprocessing phase is sensible to the choice of the initial guess for the numerical solver of the arc length minimization problem. In other words, different initial guesses may result in different outputs of the preprocessing phase. What matters to our purposes is that, according to our experiments, any such output eventually generates an acceptable curve when fed to the successive energy minimization phase.

On the other hand, to generate the closed curve examples in the following, we did not apply any preprocessing technique, but we simply selected $\phi_2^p = \cdots = \phi_{m+2}^p = 0$ and $\mathcal{Z}_0^p = \mathcal{Z}_1^p = \mathbf{0}$ as input values to be passed to the numerical procedure proposed in Subsection 5.2. Indeed, a preprocessing technique analogous to the one used in the open curve case does not yield apparent benefits on the shape of the resulting interpolant, and a different preprocessing method capable of generating a good initial guess for all possible datasets is not easily developable.

The two examples in Figure 2 show periodic quintic PH B-spline curves with $m = 9$, which interpolate 11 points on a given parametric curve. The parametric curve of the first example is $(\cos^2(u), \cos(u)\sin(u), \sin(u))$, and the one of the second example is $(5/2\cos(u) + \cos(3u),\ 5/2\sin(u) - \sin(3u),\ \sin(2u))$. In both cases the 11 interpolation points are sampled at equally spaced values $u \in [0, 2\pi]$.

Since in the closed curve case symmetry is not automatically preserved, as a future work one may devise a strategy to select more suitable angular values $\phi_2^p, \ldots, \phi_{m+2}^p$ and quaternions $\mathcal{Z}_0^p$, $\mathcal{Z}_1^p$ that could bring such an additional property to the output curve.

A simple and effective strategy to compute appropriate angular parameters and quaternions $\mathcal{Z}_0^p$, $\mathcal{Z}_1^p$, directly from the input 3D-data, could be beneficial also to the numerical procedure of the open curve case since it would eliminate the computational cost of the preprocessing phase we are currently using.

interpolants differently. minimization process (i.e., the minimization of the curvature-based functional $\hat{E}_1$), gives a visually-pleasing curve. Without such a proper initial point, the bending energy minimization algorithm could stumble into a local minimum, not producing a curve with an optimal shape. second step. However, this is superfluous because, as we can see in the next section, it is still possible to obtain a good result even if we skip the curve length minimization step.

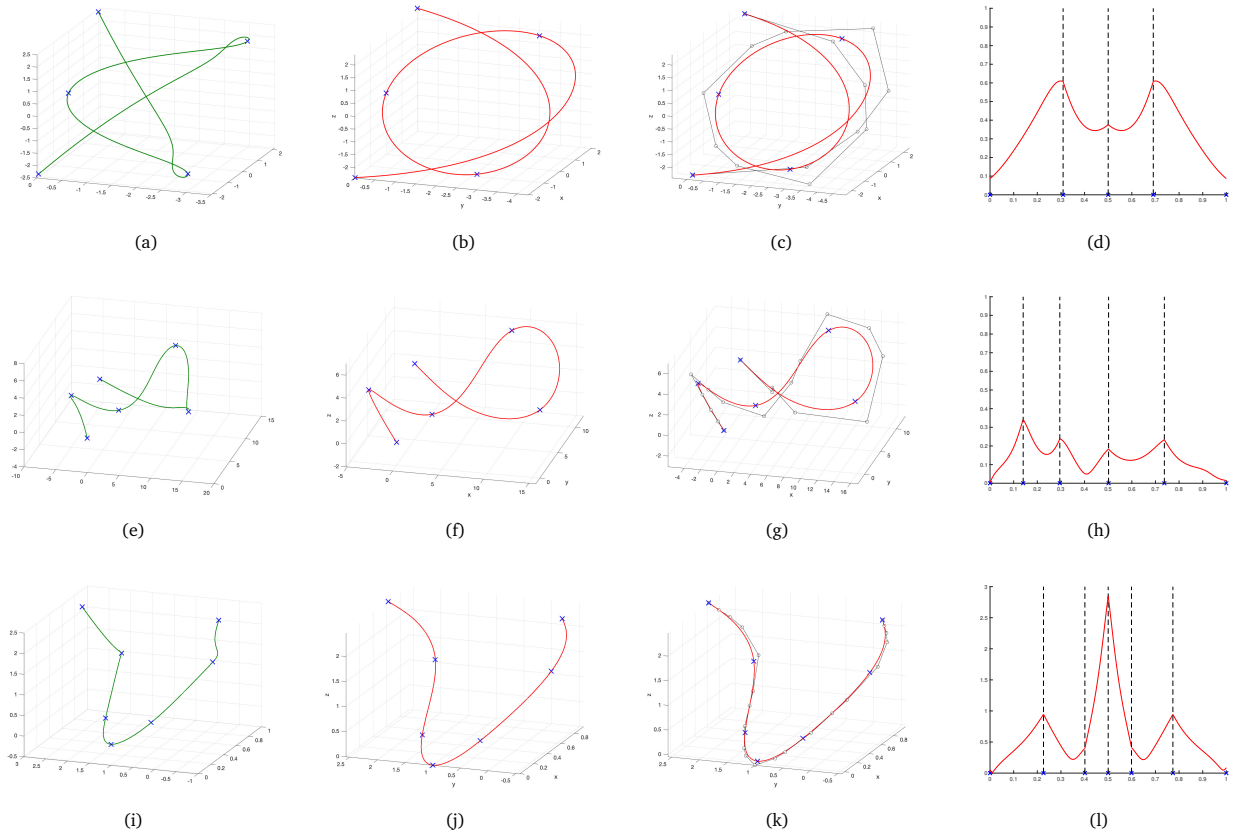

Figure 1: Examples of clamped quintic PH B-spline curves generated by our algorithm for open datasets with $m = 5, 6, 7$. In each row we display, from left to right, the curve obtained after the preprocessing phase, the final C^2 clamped quintic PH B-spline curve, its B-spline control polygon and its curvature plot.

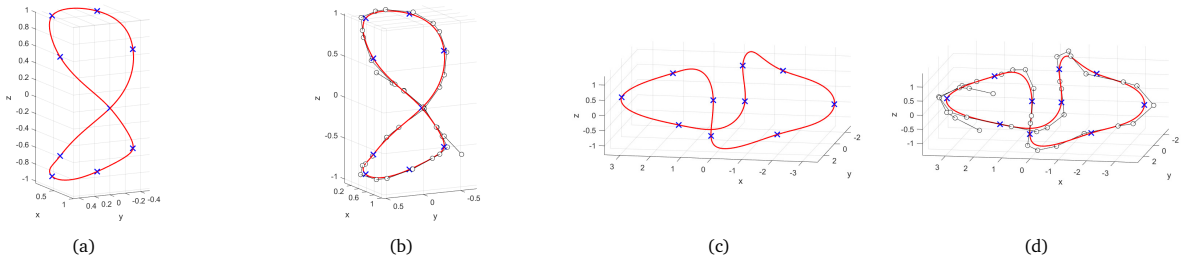

Figure 2: Examples of periodic quintic PH B-spline curves generated by our algorithm for closed datasets with $m = 9$. For each example we display from left to right the resulting C^2 periodic quintic PH B-spline curve and its B-spline control polygon.

7 Conclusion

In this paper we have investigated how to solve the C^2 interpolation problem of both open and closed spatial datasets by means of PH quintic B-spline curves. The proposed solution method offers the advantage of relying on explicit calculations, and avoids solving minimization problems subject to several nonlinear equality constraints as previously done in [2]. The leading idea is in fact to consider two initial conditions (related to the choice of $\mathcal{Z}_0$ and $\mathcal{Z}_1$) rather than an initial and a final condition as in [11], in order to give up the symmetry of the non-linear system with respect to the data and obtain a non-linear system for the coefficients of the pre-image which is easier to be solved than the quadratic non-linear system in all the quaternion unknowns that is considered in [11]. In our paper the interpolation conditions are indeed rewritten in such a way that the minimization of a functional and the successive usage of explicit quaternion formulas are enough to get the desired PH interpolant. Moreover, in our construction, the control polygon of the clamped quintic PH interpolant is made of $3m$ control points only, instead of $5m-4$ as the piecewise quintic Bézier representation used in [11] entails, and is capable of producing outputs that preserve the

symmetry of the data (see, e.g., Figure 1(d) and (l)). With respect to the clamped quintic PH interpolant proposed in [13], we can also obtain spatial curves with an improved curvature behaviour (compare Figure 1(h) with Figure 7 (right) in [13]). However, differently from the approach in [13], our method is not suited for stream interpolation since it requires the minimization of a functional depending on $\mathcal{Z}_0$ and $\mathcal{Z}_1$ but also on $\phi_2, ..., \phi_m$, which implies that the interpolation curve is produced globally and does not have a fully explicit forward local construction. Also, currently the proposed interpolation method does not guarantee that the same curve is obtained when data are reversed. One could, however, use the available free parameters to enforce this property and how to do so is a topic for future investigation.

Acknowledgements: The second and third author are members of INdAM - GNCS, which partially supported this work, as well as members of the Alma Mater Research Center on Applied Mathematics (AM^2). The research of the third author has been done within the Italian Network on Approximation (RITA) and the thematic group on "Approximation Theory and Applications" of the Italian Mathematical Union.

References

[1] G. Albrecht, C.V. Beccari, J.-C. Canonne, L. Romani. Planar Pythagorean-Hodograph B-spline curves. *Comput. Aided Geom. Design* 57 (2017) 57-77.

[2] G. Albrecht, C.V. Beccari, L. Romani. Spatial Pythagorean-Hodograph B-spline curves and 3D point data interpolation. *Comput. Aided Geom. Design* 80 (2020) 101868.

[3] G. Albrecht, C.V. Beccari, L. Romani. G^2/C^1 Hermite interpolation by planar PH B-spline curves with shape parameter. *Appl. Math. Letters* 121 (2021) 107452.

[4] B. Bastl, M. Bizzarri, K. Ferjancic, B. Kovac, M. Krajnc, M. Lavicka, K. Michalkova, Z. Sir, E. Zagar. C^2 Hermite interpolation by Pythagorean-Hodograph quintic triarcs. *Comput. Aided Geom. Design* 31(7) (2014) 412-426.

[5] M. Bizzarri, M. Lavicka, J. Vrsek. C^d Hermite interpolations with spatial Pythagorean hodograph B-splines. *Comput. Aided Geom. Design* 87 (2021) 101992.

[6] B. Dong, R. Farouki. Algorithm 952: PHquintic: A Library of Basic Functions for the Construction and Analysis of Planar Quintic Pythagorean-Hodograph Curves. *ACM Trans. on Math. Software* 41(4) (2015), article n. 28, pp 1-20.

[7] R.T. Farouki. Existence of Pythagorean-hodograph quintic interpolants to spatial G^1 Hermite data with prescribed arc lengths. *J. of Symbolic Computation* 95 (2019) 202-216.

[8] R.T. Farouki, M. al-Kandari, T. Sakkalis. Hermite interpolation by rotation-invariant spatial Pythagorean-hodograph curves. *Adv. Comput. Math.* 17 (2002) 369-383.

[9] R.T. Farouki, K. Hormann, F. Nudo. Singular cases of planar and spatial C^1 Hermite interpolation problems based on quintic Pythagorean-hodograph curves. *Comput. Aided Geom. Design* 82 (2020) 101930.

[10] R.T. Farouki, C. Giannelli, C. Manni, A. Sestini. Identification of spatial PH quintic Hermite interpolants with near-optimal shape measures. *Comput. Aided Geom. Design* 25 (2008) 274-297.

[11] R. Farouki, C. Manni, A. Sestini. Spatial C^2 PH quintic splines. In: Lyche, T., Mazure M.L., Schumaker, L. (Eds.), Curve and Surface Design: Saint-Malo 2002. Nashboro Press, Nashville, TN, pp.147-156.

[12] R.T. Farouki, C. Manni, F. Pelosi, and M.L. Sampoli. Design of C^2 spatial Pythagorean-hodograph quintic splines by control polygons. In Curves and Surfaces. Lecture Notes in Computer Science, Vol. 6920, 2012, pp. 253-269.

[13] C. Giannelli, L. Sacco, A. Sestini. Interpolation of 3D data streams with C^2 PH quintic splines. *Adv. Comput Math.* 48 (2022) 61.

[14] C. González, G. Albrecht, M. Paluszny. Visualization of dental information within CT volumes. Mathematics and Computers in Simulation 173 (2020) 71-84.

[15] C.Y. Han, H.P. Moon, S.-H. Kwon. A new selection scheme for spatial Pythagorean hodograph quintic Hermite interpolants. *Comput. Aided Geom. Design* 78 (2020) 101827.

[16] M. Huard, R.T. Farouki, N. Sprynski, L. Biard. C^2 interpolation of spatial data subject to arc-length constraints using Pythagorean-hodograph quintic splines. *Graphical Models* 76(1) (2014) 30-42.

[17] S.-H. Kwon, C.Y. Han. Spatial quintic Pythagorean-hodograph interpolants to first-order Hermite data and Frenet frames. *Comput. Aided Geom. Design* 89 (2021) 102012.

[18] L. Romani, F. Montagner. Algebraic-Trigonometric Pythagorean-Hodograph space curves. *Adv. Comput. Math.* 45(1) (2019) 75-98.

[19] L. Romani, L. Saini, G. Albrecht. Algebraic-Trigonometric Pythagorean-Hodograph curves and their use for Hermite interpolation. *Adv. Comput. Math.* 40(5-6) (2014) 977-1010.

[20] L. Romani, A. Viscardi. Construction and evaluation of Pythagorean Hodograph curves in exponential-polynomial spaces. *SIAM J. Sci. Comput.*, in press, https://doi.org/10.1137/21M1455711